Investigation of the S3 Electron Paramagnetic Resonance Signal from the Oxygen-Evolving Complex of Photosystem 2: Effect of Inhibition of Oxygen Evolution by Acetate†

Dugald J. MacLachlan and Jonathan H. A. Nugent*

Department of Biology, Darwin Building, University College London, Gower Street, London WC1E 6BT, U.K.

Received December 9, 1992; Revised Manuscript Received May 19, 1993®

ABSTRACT: An S3 electron paramagnetic resonance (EPR) signal is observed in a variety of photosystem 2 (PS2) samples in which the oxygen-evolving complex (OEC) has been inhibited. These signals have been proposed to be due to an interaction, S_2X^+, between the manganese cluster in an oxidation state equivalent to S_2 and an organic radical, either oxidized histidine [Boussac et al. (1990) *Nature 347*, 303–306] or the tyrosine radical Y_z^+ [Hallahan et al. (1992) *Biochemistry 31*, 4562–4573]. We report that treatment of PS2 with acetate at pH 5.5 leads to a slowing of the reduction of Y_z^+ and allows the trapping of an S3-type state on freezing to 77 K following illumination at 277 K. The S3 EPR signal in acetate-treated PS2 has a broader and more complex line shape but otherwise has similar properties to other S3 signals. The addition to acetate-treated samples in the S_1 state of the herbicide 3-(3,4-dichlorophenyl)-1,1-dimethylurea (DCMU), which allows only a single turnover of the reaction center, causes a large reduction in the yield of the S3 signal. Various anion and cation treatments change the S3 signal line shape and are used to show that acetate probably acts by binding and displacing chloride. We propose that a variety of treatments which affect calcium and chloride cofactor binding cause a modification of the S_2 state of the manganese cluster, slow the reduction of Y_z^+, and allow an S3 EPR signal to be observed following illumination. The origin of the S3 signal, whether a modified S_3 or S_2X^+ where X is an organic radical, remains in doubt as the involvement and identity of the organic radical is still uncertain.

In the thylakoid membrane of plants, algae and cyanobacteria, electron transfer from water to $NADP^+$ involves two photosystems, termed photosystem 1 and photosystem 2. PS2[1] is the membrane-protein complex which catalyzes electron transfer from water to plastoquinone. Absorption of light leads to photooxidation of the reaction center chlorophyll P680 and reduction of the bound plastoquinone electron acceptor Q_A via a pheophytin intermediate. These cofactors are bound to a heterodimer of polypeptides termed D1 and D2. $P680^+$ is reduced by electrons from the oxygen-evolving complex (OEC) via the intermediate Y_z. The OEC is thought to contain four manganese atoms [see Debus (1992) and Rutherford et al. (1992) for reviews]. The Mn complex probably provides both the catalytic site and the site of the charge accumulation required for water oxidation. Four turnovers of the reaction center are required to produce molecular oxygen. During its cycle, the OEC passes through five different redox states, S_0–S_4 (Kok et al., 1970), with four electrons being removed from S_0 to S_4 and O_2 being evolved between S_3 and S_0. The S_1 state is found in most centers in dark-adapted samples.

Electron transfer between the OEC and P680 is mediated by a tyrosine residue, Y_z. Y_z is tyrosine-161 of the D1 polypeptide (Debus et al., 1988b; Metz et al., 1989). A second redox-active tyrosine residue, Y_D, has been identified as tyrosine-161 of D2 (Debus et al., 1988a; Vermaas et al., 1988). Y_D^+ and Y_z^+ can be observed by EPR as Signal II ($g = 2.0045$, Hpp $\approx$ 1.9 mT). Signal II has several kinetic forms at physiological temperatures, arising from either Y_D^+ or Y_z^+. Y_z^+ and Y_D^+ can also be distinguished by their microwave power saturation characteristics, which are influenced by interaction with nearby strongly relaxing species (Warden et al., 1976; Yocum & Babcock, 1981; Styring & Rutherford, 1988).

Both Cl^- and Ca^{2+} ions act as cofactors for water oxidation [Miyao & Murata, 1984; Ghanotakis et al., 1984; see Coleman (1990) and Yocum (1991) for reviews]. These ions can only be partially substituted by similar ions, Sr^{2+} (Ghanotakis et al., 1984; Boussac & Rutherford, 1988) or Br^-, I^-, and NO_3^- [Kelley & Izawa, 1978; see Debus (1992) and Rutherford et al. (1992) for reviews]. Significant differences in ion requirements may exist between cyanobacterial and chloroplast PS2 (Debus, 1992; Pauly et al., 1992) perhaps resulting from the absence in cyanobacteria of the 17- and 23-kDa extrinsic polypeptides, which have been proposed to facilitate the retention of Cl^- and Ca^{2+} in chloroplasts. The location and number of calcium and chloride binding sites in PS2 are still unknown.

Recently new EPR signals attributed to the OEC have been detected at cryogenic temperatures in PS2 depleted of Ca^{++} or Cl^-. Boussac et al. (1989) investigated PS2 calcium-depleted by NaCl washing and then reconstituted with the 17- and 23-kDa polypeptides. The reconstituted PS2 was shown to have an unusually dark-stable, modified multiline signal ($g = 1.98$, >26 lines spread over 160 mT, $t_{1/2}$ several hours). The signal was removed by addition of Ca^{++}. This dark-stable multiline signal was assigned to a modified form

† We acknowledge financial assistance from the U.K. Science and Engineering Research Council.

* Address correspondence to this author.

® Abstract published in *Advance ACS Abstracts,* August 15, 1993.

[1] Abbreviations: EPR, electron paramagnetic resonance spectroscopy; DCMU, 3-(3,4-dichlorophenyl)-1,1-dimethylurea; PPBQ, phenyl-1,4-benzoquinone; OEC, oxygen-evolving complex; PS2, photosystem 2; MES, 2-(*N*-morpholino)ethanesulfonic acid; Chl, chlorophyll; Hpp, peak to trough line width of EPR spectrum; ADRY, accelerating the deactivation reactions of the OEC; FCCP, carbonyl cyanide *p*-(trifluoromethoxy)-phenylhydrazone.

0006-2960/93/0432-9772$04.00/0

of the normal S_2 state which gives rise to a multiline signal (>18 lines) centered at $g = 2$ and is attributed to a mixed valence Mn cluster in a $S' = 1/2$ ground state (Dismukes & Siderer, 1980). The S_2 state can also give rise to an EPR signal centered at $g = 4.1$ attributed to a mixed-valence Mn tetramer in an $S' > {}^1/_2$ state (Casey & Sauer, 1984; Haddy et al., 1992).

Illuminating at 273 K and then freezing the calcium-depleted PS2 samples resulted in loss of the modified multiline and the generation of a 16.4-mT-wide EPR signal split around the $g = 2$ region, which was assigned to an S_3 state (Boussac et al., 1989), referred to here as S3. This was supported by experiments showing the appearance of the signal following a single laser flash to a sample in the modified S_2 state (Boussac et al., 1990b). It was later shown that the presence of the 17- and 23-kDa extrinsic polypeptides was not necessary for the generation of the modified S_2 or S3 signals but that EDTA, EGTA, or citrate was required in order to observe the dark-stable multiline (Ono & Inoue, 1990b; Boussac et al., 1990a). Similar EPR signals were observed in samples calcium-depleted by citrate treament (Sivaraja et al., 1989; Ono & Inoue, 1990a,b). The S3 signal can also be formed in PS2 from the cyanobacterium *Synechocystis* following washes in Ca^{++}-free buffer containing EGTA (Kirilovsky et al., 1992).

The detection of S3 EPR signals is not limited to calcium-depleted samples, as shown by the observation of a similar signal in chloride-depleted or fluoride-treated preparations (Baumgarten et al., 1990; Boussac et al., 1992) and in ammonia-treated PS2 (Hallahan et al., 1992; Andreasson & Lindberg, 1992). The S3-type signals in chloride-depleted, fluoride-treated, ammonia-treated, and *Synechocystis* samples have some distinct character, such as decreased splitting, which indicates different structural properties between these and calcium-depleted chloroplast PS2 samples.

Acetate treatment of PS2 has been shown to affect both electron donor and acceptor sites in PS2 (Sinclair, 1984; Sandusky & Yocum, 1986). Acetate inhibits electron flow between Q_A and Q_B, in a manner analogous to formate, by competing with bicarbonate binding to a site near the non-heme iron located between the two quinones (Stemler & Murphy, 1985; Blubaugh & Govindjee, 1988). Displacement of bicarbonate by acetate or formate causes a shift in the g-value of the Q_A iron semiquinone EPR signal from $g = 1.9$ to near $g = 1.8$ (Vermaas & Rutherford, 1984; Nugent et al., 1992).

High concentrations of acetate ions (>100 mM) have also been shown to inhibit water oxidation reversibly in the cyanobacterium *Synechococcus*, retarding the reduction kinetics of $P680^+$ by the OEC (Saygin et al., 1986). Following inhibition by acetate, two electrons were available from the donor side. It has been suggested that acetate competes with chloride binding (Sinclair, 1984; Saygin et al., 1986). As chloride concentration increased, the amount of acetate required for inhibition at pH 5.5 rose from 200 mM in the presence of 1 mM chloride to 660 mM in the presence of 15 mM chloride. Addition of chloride to treated samples restored oxygen evolution (Saygin et al., 1986). In room-temperature EPR studies on acetate-treated samples, Bock et al. (1988) using *Synechococcus* PS2 observed a slowing of Y_z^+ reduction and also detected a 1.4-mT radical near $g = 2$ which was attributed to $P680^+$. Using ADRY reagents, which destabilize higher oxidation states of the OEC (Renger, 1972; Ghanotakis et al., 1982; Hanssum et al., 1985), the optical spectrum of Y_z/Y_z^+ was obtained in acetate-treated samples (Gerken et al., 1989).

It has been proposed that during the S_2–S_3 transition, an oxidation of a histidine residue close to the manganese cluster occurs, the interaction giving rise to the S3 signal (Boussac et al., 1990b). Boussac et al. (1990b) correlated their EPR data to the possible histidine oxidation by using transient absorption spectroscopy. This view was challenged by Hallahan et al. (1992), who suggested that an interaction between Y_z^+ and S_2 could also account for the S3 signal. The proposal that histidine oxidation occurred was recently defended (Boussac & Rutherford, 1992).

We have investigated the properties of the S3 EPR signal obtained in PS2 treated with acetate. This has enabled the development of an easy method for investigation of anion and cation effects on PS2, which has then been used to study their effect on S3 states. This allows discussion of the recent opposing papers (Hallahan et al., 1992; Boussac & Rutherford, 1992) and reaffirms the view that the case for histidine oxidation is not proven. This work was briefly discussed in MacLachlan et al. (1992).

MATERIALS AND METHODS

Buffers containing MES and sucrose were treated with Chelex prior to the addition of NaCl and EGTA to remove any calcium impurities. All samples were stored at 77 K before use.

PS2 membranes (BBYs, Berthold et al., 1981; P680/Chl 1:225–250, Chl *a*/Chl *b* ratio 2.05–2.20:1) were prepared from market spinach by the modified method of Ford and Evans (1983) and were depleted of Ca^{++} according to a modified method of Boussac et al. (1989) as given in Hallahan et al. (1992). These EGTA/salt-washed PS2 membranes will be referred to as calcium-depleted for simplicity, although the extent of calcium depletion is still a matter of controversy [see Debus (1992) for discussion]. The calcium-depleted PS2 membranes were collected by centrifugation or further dialyzed against 0.3 M sucrose and 20 mM MES for 3 h in the dark, in order to reconstitute the 17- and 23-kDa extrinsic polypeptides. The membranes were centrifuged at 40000*g* for 30 min and resuspended in 0.3 M sucrose, 20 mM MES, 10 mM NaCl, and 100 μM EGTA, pH 6.5.

Sodium acetate- or salt-treated PS2 was prepared from PS2 membranes by resuspending the membranes in 40 mM MES, pH 5.5. The membranes were centrifuged at 40000*g* for 20 min and finally resuspended in the dark using the same buffer containing 0.3 M sucrose and the sodium acetate or other salt at the concentration given in the text. This method of resuspension in the final treatment buffer at pH 5.5 was used in preference to direct addition of specific concentrations of sodium acetate to the PS2 samples. The latter method causes problems associated with the buffering effects of high concentrations of acetate which result in variations in pH with acetate concentration. The resuspension method results in samples of slightly differing chlorophyll concentration. In some samples as noted in the text, following 30 min of sodium acetate treatment (600 mM), the sample was dialyzed against 0.3 M sucrose and 40 mM MES, pH 5.5, containing 10 mM sodium acetate to give treated samples with a low concentration of acetate.

The membranes obtained and used as a result of the calcium depletion and sodium acetate treatments were depleted of greater than 90% of their oxygen-evolving activity. This was measured in a Clark-type oxygen electrode at 298 K using ferricyanide and PPBQ as electron acceptors. The control was depleted membranes to which 20 mM calcium chloride was added; the sample was then incubated for 30 min on ice.

Ammonia-treated samples at pH 7.5 were prepared as in Hallahan et al. (1992) in the presence of high chloride concentrations. For EPR, samples contained 1 mM PPBQ and 100 mM NH_4Cl to give a free base NH_3 concentration of 2 mM (Britt et al., 1989). To increase the number of reaction centers to which the slow-binding ammonia is bound, dark-adapted samples were "annealed" [see Britt et al. (1989)] as in Hallahan et al. (1992). A similar yield of S3 was obtained if 250 K illumination replaced annealing and 277 K illumination (Andreasson & Lindberg, 1992).

EPR Spectrometry. For EPR at cryogenic temperatures, 0.3-mL samples (at approximately 8 mg of Chl/mL) were placed in 3-mm-diameter EPR tubes. The Chl/PS2 ratio (175–225) of samples was also determined by spin quantitation of the Y_D^+ EPR signal using potassium nitrosodisulfonate as spin standard, as given in Buser et al. (1992). Samples were treated as described in the figure legends and then dark-adapted for a further 30 min before being frozen to 77 K. Additions of DCMU and PPBQ were made from freshly made concentrated stock solutions in dimethyl sulfoxide. FCCP was used from a stock solution in ethanol. To obtain the S3 signal, samples were illuminated at 277 K for 30 s using an unfiltered 650-W light source (1000 $\mu E\ m^{-2}\ s^{-1}$) and then frozen to 77 K under illumination. During dark adaptation, samples were kept on ice at 273 K.

Identical sets of samples in calibrated EPR tubes were made for each experiment, using the same preparation and similar chlorophyll concentration. Using the signals present in control samples (cytochrome b_{559}, etc.) the EPR spectrometer and measurement conditions were calibrated for experiments which involved EPR data collection on different days. Spectra shown which compare acetate and salt-treated samples are not corrected for the minor differences in chlorophyll concentration (±20%) which occurred as a result of the preparative method (see above).

EPR spectrometry was performed using a Jeol RE1X spectrometer fitted with an Oxford Instruments liquid helium cryostat. EPR conditions are given in the figure legends. It should be noted that in order to observe hyperfine structure, we use different EPR conditions (principally a lower microwave power, modulation amplitude, and response time) than other groups. Spectra of greater signal to noise and identical to those of Boussac and Rutherford (1992) were obtained if their conditions were used. For room-temperature EPR, 10- or 15-μL samples in glass capillary tubes were placed inside EPR tubes. These samples were run as above using the cavity fitted to the Oxford Instruments cryostat. Spectra were recorded and manipulated using a Dell microcomputer running Asyst software.

$P_{1/2}$ (the microwave power for half-saturation) was determined graphically as in Styring and Rutherford (1988) from a plot of log $(I/\sqrt{P})$ vs log P, where P is the microwave power and I is the signal amplitude. $P_{1/2}$ is found by extrapolating the initial ($P \ll P_{1/2}$) and final ($P \gg P_{1/2}$) linear sections of the curves to their point of intersection, which is the $P_{1/2}$ value.

RESULTS

Organic Radicals Observed at Room Temperature. In the presence of a functioning OEC, the reduction of Y_z^+ is normally too fast to allow observation of the species attributed to Y_z^+ using conventional EPR. As shown previously for sodium acetate-treated samples (Bock et al., 1988) the kinetics of Y_z^+ reduction are slowed, enabling the Y_z^+ radical to be detected on illumination at room temperature (Figure 1).

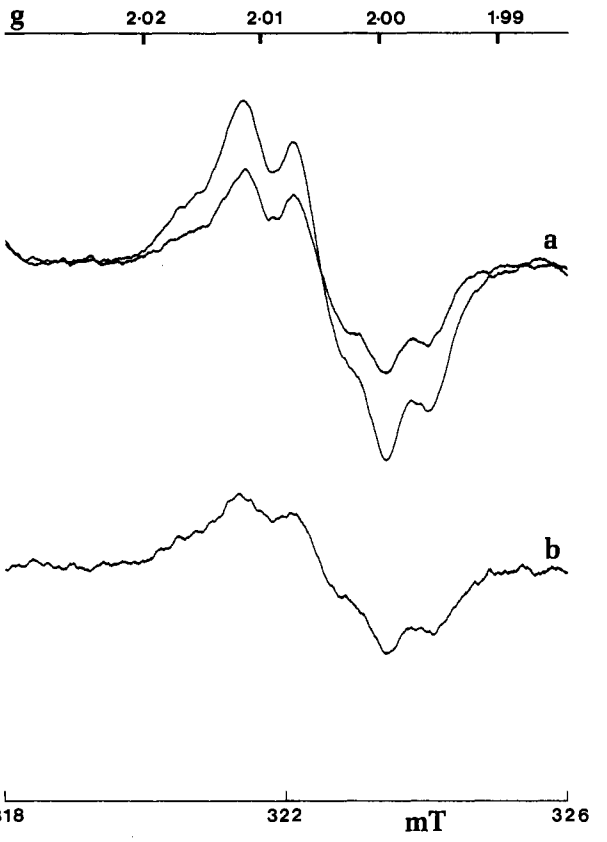

FIGURE 1: EPR spectra of tyrosine radicals at room temperature in 500 mM sodium acetate-treated PS2 at pH 5.5. Sample contains 1 mM ferricyanide and 1 mM ferrocyanide as electron acceptor, 40 mM MES, and 0.3 M sucrose. (a) (outer line) Sample during illumination at 295 K and (inner line) in the dark following illumination (inner line showing Y_D^+). (b) Difference spectrum (light on – dark) showing light-induced Y_z^+. EPR conditions: microwave power 20 mW, modulation width 0.25 mT.

Figure 1a (inner line) shows the $g = 2$ EPR spectrum at 295 K of a sodium acetate-treated sample in the dark, 10 min after illumination (which was the time required to acquire the spectrum). This is the spectrum of Y_D^+, the stable tyrosine radical. It has a measured line width of 1.95 mT and has a $P_{1/2}$ of about 25 mW. On illumination (Figure 1a, outer line), Y_z^+ (identified by a $P_{1/2} > 50$ mW) was formed within the time constant of the spectrometer, superimposed on the spectrum of Y_D^+. No radical other than Y_D^+ and Y_z^+ was detected. Y_z^+ (Figure 1b) has a line width in the sodium acetate-treated samples of 2.02 mT, similar to that found in calcium-depleted samples (2.03 mT; Hallahan et al., 1992) and slightly broader than Y_D^+. The larger $P_{1/2}$ for Y_z^+ shows that it is undergoing spin relaxation by a neighboring paramagnet, a situation previously observed for Y_z^+ in native or ammonia-treated PS2 (Warden et al., 1976; Yocum & Babcock, 1981). When calcium chloride was added to the acetate-treated samples followed by incubation for 20 min at 273 K, the yield of Y_z^+ was greatly diminished.

The major cause of slow changes to Y_D^+ in the dark in untreated PS2 samples is the oxidation of S_0 to S_1 by Y_D^+ (Vermass et al., 1984; Styring & Rutherford, 1987). Changes in Y_D^+ during the short dark period may affect quantitation of the Y_z^+ produced. Illuminated and dark-adapted spectra were recorded after a 20-min incubation with 20 mM calcium chloride and compared to spectra taken of the same sample before addition of calcium chloride. We conclude that there was instability of Y_D^+ as a result of sodium acetate treatment and that this loss of Y_D^+ was increased following further

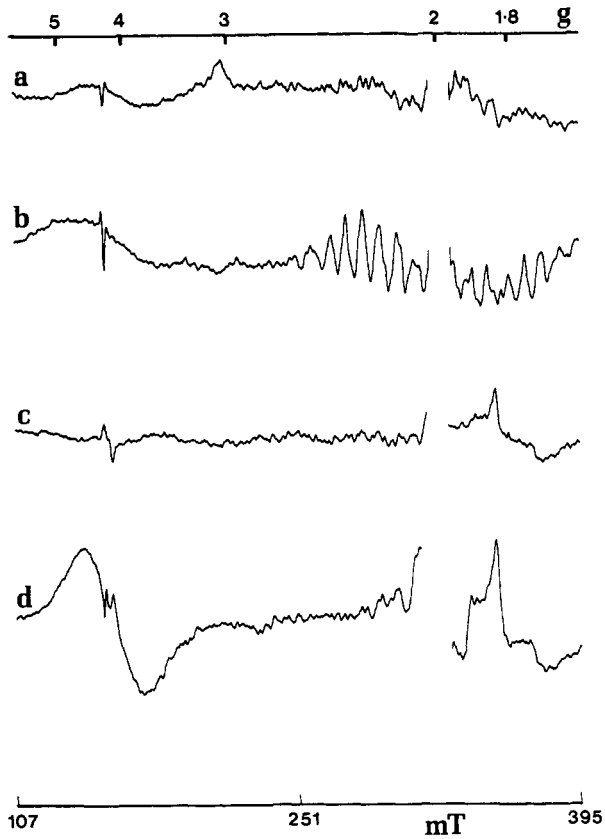

FIGURE 2: EPR spectra comparing the effects of illumination on untreated and sodium acetate-treated PS2 samples at pH 5.5. All samples contain 0.5 mM PPBQ, 40 mM MES, and 0.3 M sucrose. (a) Untreated PS2, illuminated at 77 K for 5 min with the dark-adapted spectrum (30 min, 273 K) subtracted. (b) Untreated PS2, illuminated at 200 K for 10 min with a 77 K illuminated spectrum (a) subtracted. (c) Sodium acetate-treated (500 mM) PS2, illuminated at 200 K for 10 min with a 77 K illuminated spectrum subtracted. (d) Sodium acetate-treated (500 mM) PS2 containing 250 μM FCCP, illuminated at 277 K for 30 s and then frozen under illumination to 77 K. The spectrum of the 30-min, 273 K dark-adapted sample has been subtracted. EPR conditions: microwave power 10 mW, modulation amplitude 1.6 mT, temperature 8 K. The sharp feature at $g = 4.3$ is an artifact from subtraction of the large $g = 4.3$ signal from rhombic iron present in the samples.

illumination. This slow decay of Y_D^+ (typically 30–50% decrease in 120 min) made quantitation of the tyrosine radicals uncertain.

The room-temperature data support earlier work (Bock et al., 1988) that sodium acetate-treated samples can transfer electrons from Y_z to the electron acceptors of PS2. Therefore, the electron transfer chain between P680 and Y_z remains competent after sodium acetate treatment and the point of inhibition lies between Y_z and the OEC. The ability of calcium chloride to decrease the yield of Y_z^+ suggests that these ions restore Y_z^+ reduction by the OEC.

Instability of Y_D^+ has been observed in other studies and may be a result of chloride depletion, as this effect was previously noted in chloride-depleted PS2 (Damoder et al., 1986) and PS2 treated at pH 8.3 (Lockett et al., 1990). The affinity for chloride is lower at alkaline pH (Theg & Homann, 1982; Homann, 1988), probably through deprotonation of a ligand at the binding site. Effective acetate treatment requires an acidic pH (see below), suggesting that either the protonation of acetate or the binding site, or both, is required for chloride displacement by acetate.

EPR of Sodium Acetate-Treated Samples at Cryogenic Temperatures. Figure 2 compares untreated (a,b) and sodium acetate-treated (c,d) samples both poised at pH 5.5. Figure 2a shows the effect of illuminating untreated PS2 at 77 K. A small yield of $g = 4.1$ S_2 signal is obtained but the major electron donor is cytochrome b_{559} giving signals near $g = 3$ (g_z) and $g = 2.2$ (g_y). The reduction of Q_A is shown by the $g = 1.9$ signal of the iron semiquinone. Figure 2b shows the effect of 200 K illumination on untreated PS2 at pH 5.5. The OEC replaces cytochrome b_{559} as the electron donor and both forms of S_2, the $g = 4.1$ and the multiline signal centered near $g = 2$ are obtained.

In sodium acetate-treated samples at pH 5.5, 77 or 200 K illumination does not produce any signals attributable to the OEC. Inhibition of formation of the multiline signal at 200 K by 50 mM sodium acetate at pH 7.5 has previously been observed (Ono et al., 1987). As shown in Figure 2c, the Q_A iron semiquinone signal is changed to the $g = 1.8$ form by acetate. Acetate treatment also changes the availability of electron donors such as cytochrome b_{559} at 77 K, resulting in a lower yield of Q_A^- at 77 K than at 200 K. This is revealed by the appearance of some Q_A^- in the difference spectrum, Figure 2c.

Evidence that the S_2 state could be observed in sodium acetate-treated samples is shown in Figure 2d, where samples containing the ADRY reagent FCCP (250 μM) allow formation of the $g = 4.1$ S_2 state by freezing under illumination. FCCP accelerates the deactivation of S states above S_1 in untreated PS2 at physiological temperatures (Renger, 1972; Ghanotakis et al., 1982; Hanssum et al., 1985). This result therefore indicates that the formation of the S_2 state is not inhibited by acetate treatment. The high salt concentration present during the acetate treatment affects the binding of the 17- and 23-kDa polypeptides [not shown but see Debus (1992) for review], perhaps leading to these effects. However, the $g = 4.1$ signal has been reported to be absent in PS2 lacking the 17- and 23-kDa extrinsic polypeptides (dePaula et al., 1986) unless Sr^{2+} was present (Boussac & Rutherford, 1988), suggesting that a more specific effect of sodium acetate on the OEC occurs.

The line width of the $g = 4.1$ signal in Figure 2d at about 30 mT is narrower than that found in native samples but similar to that found in fluoride- or ammonia-treated samples [see Rutherford et al. (1992) and Debus (1992) for reviews]. Further experiments using oriented PS2 preparations are needed to investigate if hyperfine structure, similar to that found in ammonia-treated samples (Kim et al., 1992), can be detected.

No evidence for a dark-stable S_2 multiline was found in acetate-treated samples. The presence of a chelator, either EGTA or citrate, was required in order to observe this signal in calcium-depleted preparations (Ono & Inoue, 1990b; Boussac et al., 1990a). Addition of EGTA or EDTA to sodium acetate-treated samples did not allow formation of a dark-stable multiline following illumination at 277 K.

Formation of the S3 Signal at Cryogenic Temperatures. Illumination of a sodium acetate-treated sample at 277 K and then freezing under illumination to 77 K causes the appearance of the signal split around $g = 2$, attributed to an S3 state (Figure 3a). The signal was present in greater yield in samples containing >100 mM sodium acetate. The signal was also obtained in PS2 samples treated with 600 mM sodium acetate that were dialyzed against 40 mM MES and 10 mM acetate, pH 5.5, to lower acetate concentration in the absence of chloride. This would be expected to reconstitute any unbound extrinsic polypeptides, as happens during dialysis of salt-treated PS2. Therefore the conditions producing the signal indicate specific effects of the acetate on PS2.

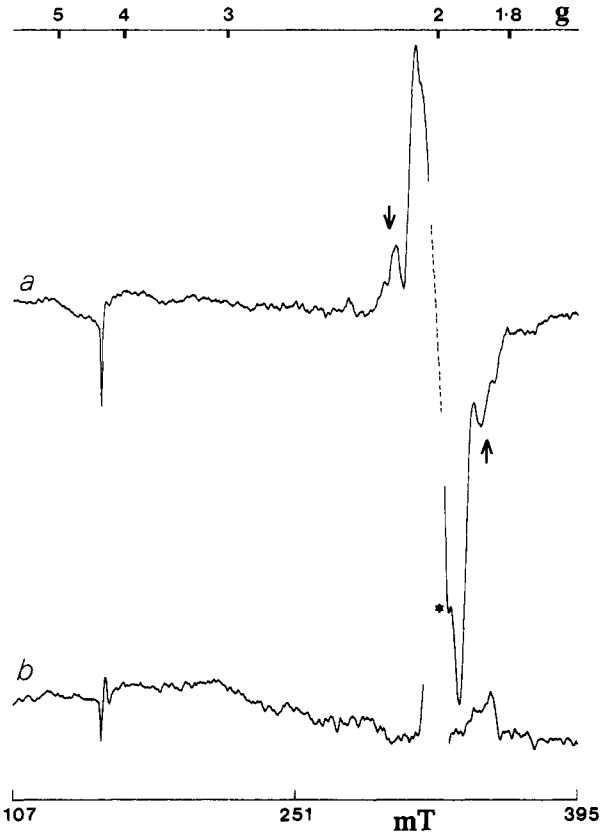

FIGURE 3: EPR spectra comparing the yield of the S3 signal in sodium acetate-treated PS2 samples. (a) With 0.5 mM PPBQ and (b) with 0.5 mM DCMU. Paired samples were sodium acetate-treated (500 mM) at pH 5.5, DCMU or PPBQ was added, and the sample was stored in the dark at 77 K. The samples were illuminated at 277 K for 30 s and then frozen under illumination to 77 K. The spectrum of the 30-min, 273 K dark-adapted sample has been subtracted. EPR conditions: microwave power 5 mW, temperature 10 K, modulation amplitude 1.6 mT. The large signal at $g = 2$ from tyrosine radicals has been removed; the dotted line shows which spectra are joined and is not intended to suggest the $g = 2$ line shape. The peaks arrowed and marked with an asterisk are discussed in the text.

Many studies have shown a requirement for an exogenous electron acceptor, PPBQ, in order to obtain a high yield of S3 (Boussac et al., 1989; Tso et al., 1991; Hallahan et al., 1992). About 50–70% of the maximum yield of S3 signal was obtained in sodium acetate-treated samples without addition of exogenous acceptor. The addition of PPBQ was required to achieve maximum signal size (Figure 3a). Addition of 0.5 mM DCMU, restricting the reaction center to a single turnover on 277 K illumination, almost completely abolished the ability to generate the S3 signal (Figure 3b). The yield of S3 was also greatly decreased by FCCP treatment (Figure 2d). This suggests that the OEC is in S_1 (or lower S state) in dark-adapted samples. Saygin et al. (1986) and Bock et al. (1988) have shown that two turnovers of the reaction center can occur from an S_1 state in dark-adapted acetate-treated samples. This would allow S3 (either by oxidation of the manganese cluster or by formation of S_2X^+, where X is an organic radical) to be reached in samples containing PPBQ but only S_2 to be formed in samples containing DCMU.

We have shown previously (Hallahan et al., 1992) that the S3 signal was greatly reduced in size in calcium-depleted PS2 that had been treated with 0.5 mM DCMU prior to freezing to 77 K under illumination. This effect of DCMU has been recently challenged (Boussac & Rutherford, 1992) despite the authors of that paper obtaining a 50% reduction in yield using a lower DCMU concentration (100 vs 500 μM) than Hallahan et al. (1992). The decreased yield of S3 which does occur in calcium-depleted samples in the presence of DCMU is due to the backreaction between Q_A^- and OEC, which is maximized by DCMU blocking Q_A^- to Q_B electron transer and minimized by allowing PPBQ to reoxidize Q_A^-. This results in a decreased yield of S3 with DCMU even though the calcium-depleted samples have a dark-stable S_2 state.

Characteristics of the S3 Signal in Sodium Acetate-Treated PS2. The S3 signal formed in sodium acetate-treated samples had microwave power saturation and temperature dependence characteristics ($P_{1/2}$ approximately 5 mW, temperature optimum 10–20 K) similar to other forms of the S3 signal discussed above (Boussac et al., 1989; Baumgarten et al., 1990; Hallahan et al., 1992; Andreasson & Lindberg, 1992), indicating fast relaxation by a transition metal. The rate of decay of S3 following illumination at 277 K had a $t_{1/2}$ of 15 s, faster than calcium-depleted samples reconstituted with extrinsic polypeptides but similar to unreconstituted calcium-depleted PS2 (Boussac et al., 1990a; Hallahan et al., 1992).

As found with calcium-depleted PS2 (Hallahan et al., 1992) when acetate-treated PS2 was frozen under illumination to trap the S3 signal and the sample was then stored at 77 K in the dark, the S3 signal partially decayed and could be restored by 77 K illumination. The extent of decay of the S3 signal varied between PS2 preparations. Presumably this occurs by reduction of the putative oxidized organic radical or manganese cluster at 77 K by either PS2 electron acceptors or another redox component. No multiline S_2 EPR signal was detected in partially decayed samples.

Incubations of acetate-treated PS2 at various pH values revealed that the formation of the S3 signal was sensitive to pH, with the yield of S3 being lowered to approximately 50% at pH 6.5 compared to pH 5.5 and greatly decreased by pH 7.5. No marked pH dependence in the splitting of the peaks was noted. This confirms that a high concentration of acetate is not the sole requirement and that the protonated form of acetate and/or a pH effect on the binding site is required for the effect to occur.

On formation and trapping of S3, an increased amplitude of the tyrosine radical at $g = 2$ was observed at cryogenic temperatures and higher microwave powers (>1 mW) (not shown), indicating trapping of Y_z^+ or changes in the relaxation behavior of Y_D^+ [see Hallahan et al. (1992) and Boussac and Rutherford (1992)]. A small but variable yield of a $g = 2$ radical attributed to chlorophyll [see Miller and Brudvig (1991)] was also trapped by this procedure.

Comparison of the Different Line Shapes of S3 EPR Signals. Figure 4 compares the line shape of S3 signals in NaCl-washed PS2 (Figure 4a) and acetate-treated PS2 (Figure 4b–e). The S3 signal in acetate-treated PS2 has a greater line width (Hpp) between the major peaks (23 ± 2 mT compared to 16 mT) and a more complex line shape. A comparison of the areas of the S3 signals (obtained by integration) from NaCl-washed and acetate-treated PS2 at the same chlorophyll concentration revealed a similar yield of S3.

To assign the outer lines (arrowed in Figures 3 and 4) to the S3 signal in acetate-treated samples, other PS2 EPR signals have to be eliminated. Q_A iron semiquinone signals interfere in the high-field region. In the low-field region the g_y peak of cytochrome b_{559} may interfere, but this can be ruled out as no corresponding changes occur at the g_z position near $g = 3$. Careful analysis of a number of samples and EPR conditions lead us to conclude that the outer lines shown in Figure 4 may be part of the S3 line shape. The outer lines

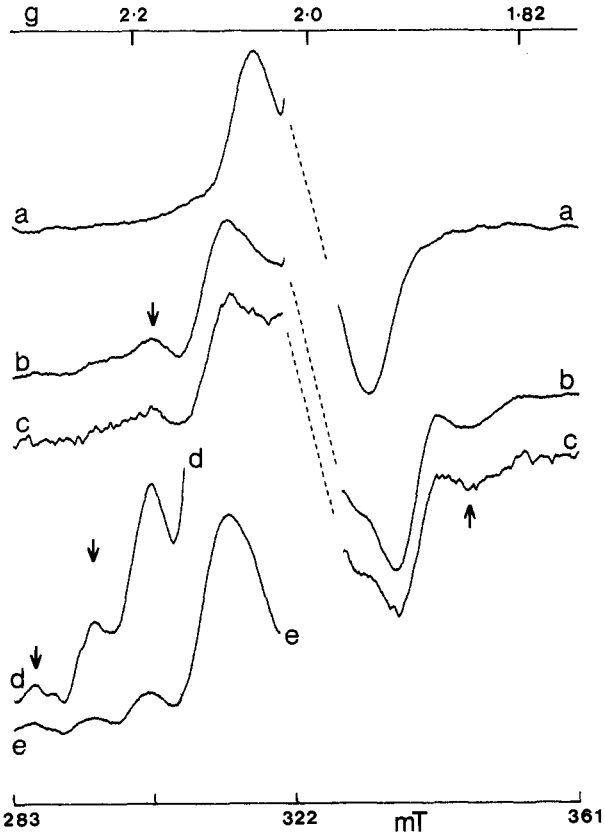

FIGURE 4: EPR spectra showing the line shape properties of the S3 signal at cryogenic temperatures. (a) An NaCl-washed, calcium-depleted sample reconstituted with extrinsic polypeptides, pH 6.5, containing 5 mM EGTA and 0.5 mM PPBQ. (b) Sodium acetate-treated PS2 (500 mM), 8 mg of Chl/mL, pH 5.5, containing 0.5 mM PPBQ, microwave power 5 mW. (c) Same as in (b) but microwave power 10 μW. (d) Same as in (b) but concentrated sample (~20 mg/mL), modulation amplitude 2 mT, and gain 250. (e) Same as in (d) but gain 50. The samples were illuminated at 277 K for 30 s and then frozen under illumination to 77 K. The spectrum of the 30-min, 273 K dark-adapted sample has been subtracted. Other conditions were as in Figure 3.

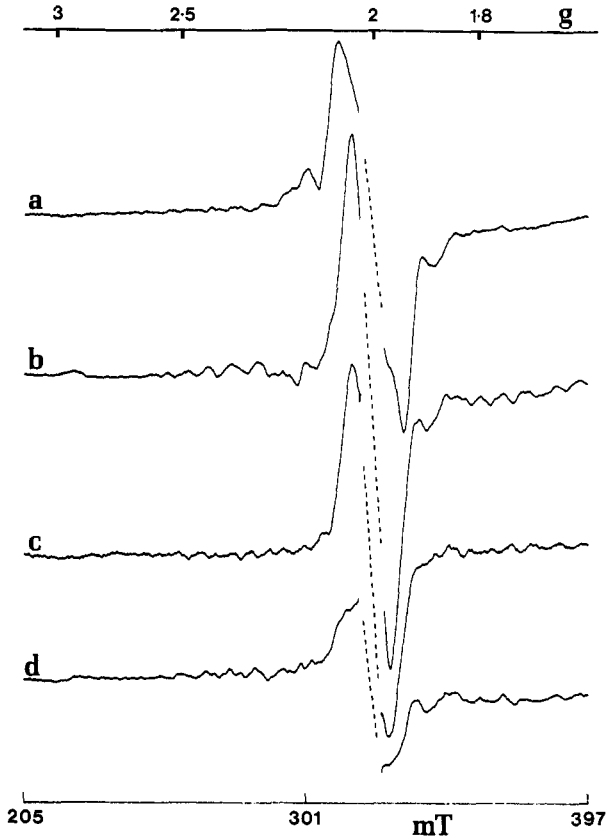

FIGURE 5: Comparison of S3 line shapes after acetate and chloride treatment. Salt-treated PS2 samples containing 0.5 mM PPBQ, 0.3 M sucrose, and 40 mM MES at pH 5.5 were prepared with the additions given below as shown in Materials and Methods. Samples were illuminated for 30 s and frozen under illumination to 77 K, and the 30-min, 273 K dark-adapted spectrum was substracted to give the difference spectrum shown. Samples also contained (a) 600 mM sodium acetate, (b) 600 mM sodium chloride, (c) 300 mM sodium acetate plus 300 mM sodium chloride, and (d) 300 mM sodium acetate plus 100 mM calcium chloride. Spectrum d was recorded on twice the gain of spectra a–c; other EPR conditions were as in Figure 3.

were present when the S3 signal was observed at a variety of microwave powers and temperatures (Figure 4b–e) and are clearly resolved with improved signal to noise using more concentrated samples (Figure 4d,e). In some spectra an inner line was observed, especially on the high-field side of $g = 2$ (indicated by an asterisk in Figure 3), suggesting superposition of S3 signals of different line widths in these samples.

Acetate treatment has been proposed to exert its effect by replacing or displacing chloride from its binding site(s) in the QEC (Sinclair, 1984; Saygin et al., 1986; Bock et al., 1988). Measurements of oxygen evolution by our acetate-treated samples confirmed a severe >90% inhibition which was largely removed by addition of chloride, although subsequent addition of Ca^{++} induced a further increase in rate, suggesting some depletion of calcium. A chloride displacement/replacement by acetate could also explain the lack of multiline signals as this signal has been reported to be suppressed in chloride-depleted samples (Ono et al., 1986; de Paula et al., 1986; Boussac & Rutherford, 1992). The effect of acetate treatment on chloride and calcium cofactors was therefore investigated by comparing the line shape and yield of the S3 signal following treatment with various cation acetates and chlorides (Figures 5 and 6).

Figure 5 compares the effects of sodium acetate (Figure 5a) and sodium chloride (Figure 5b) and shows that in the presence of chloride ion, either by itself (Figure 5b) or mixed with acetate (Figure 5c), the S3 signal has a line width (13-16 mT) more characteristic of calcium-depleted samples. A low yield of the multiline S_2 signal was also observed in chloride-containing samples. Clearly chloride removes the effect of acetate on the S3 line shape, with the high sodium chloride concentration giving similar conditions to those used to cause calcium depletion. Addition of calcium chloride to a sodium acetate-treated sample allows formation of S3 but in greatly decreased yield, as expected if chloride and acetate compete for binding. A low yield of S3 was obtained by washing and resuspension in 40 mM MES buffer, pH 5.5, alone (not shown). This is probably to be expected as partial chloride depletion is slowly achieved by a similar procedure although at higher pH (Damoder et al., 1986). There are therefore two effects of pH, one resulting from a direct pH effect on cofactor binding and one which affects the potency of acetate treatment.

Figure 6 shows the effect of divalent cations on the properties of the S3 signal. Magnesium acetate treatment (Figure 6b) gave an S3 signal similar to that obtained by sodium acetate treatment (Figure 5a). Calcium acetate (Figure 6a) gave a signal of similar line width but with sharper resolution of peaks. This spectrum reflects the affect of acetate while minimizing calcium depletion, which may occur at high salt concentrations. Addition of magnesium acetate and chloride (Figure 6c) reduced the line width to 15 mT in a result similar to that seen for sodium chloride (Figure 5c). Addition of

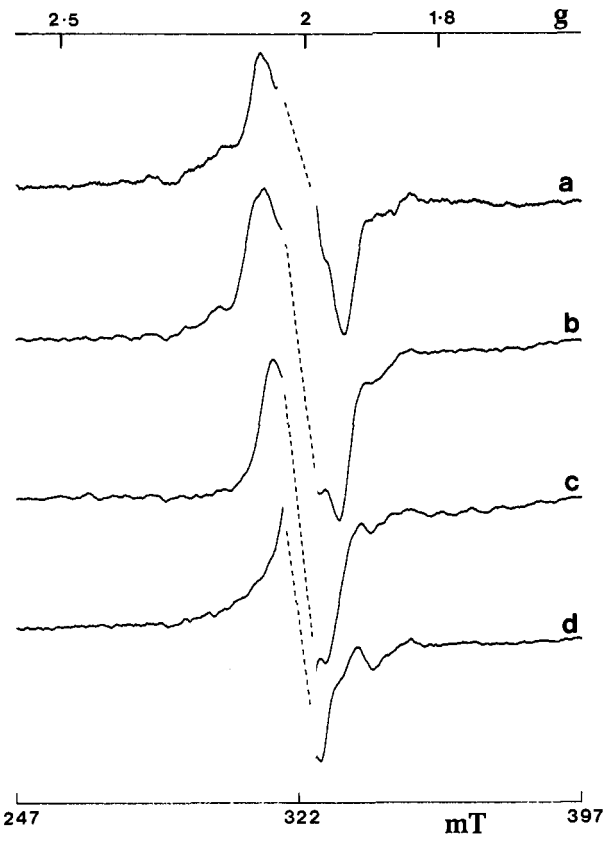

FIGURE 6: Comparison of S3 line shapes after cation treatments. Salt-treated PS2 samples containing 0.5 mM PPBQ, 0.3 M sucrose, and 40 mM MES at pH 5.5 were prepared as given in Figure 5 and Materials and Methods. Samples were illuminated for 30 s and frozen under illumination to 77 K, and the 30-min, 273 K dark-adapted spectrum was subtracted to give the difference spectrum shown. Samples contained (a) 300 mM calcium acetate, (b) 300 mM magnesium acetate, (c) 150 mM magnesium acetate plus 150 mM magnesium chloride, and (d) 300 mM magnesium acetate plus 100 mM strontium chloride. EPR conditions were as in Figure 3.

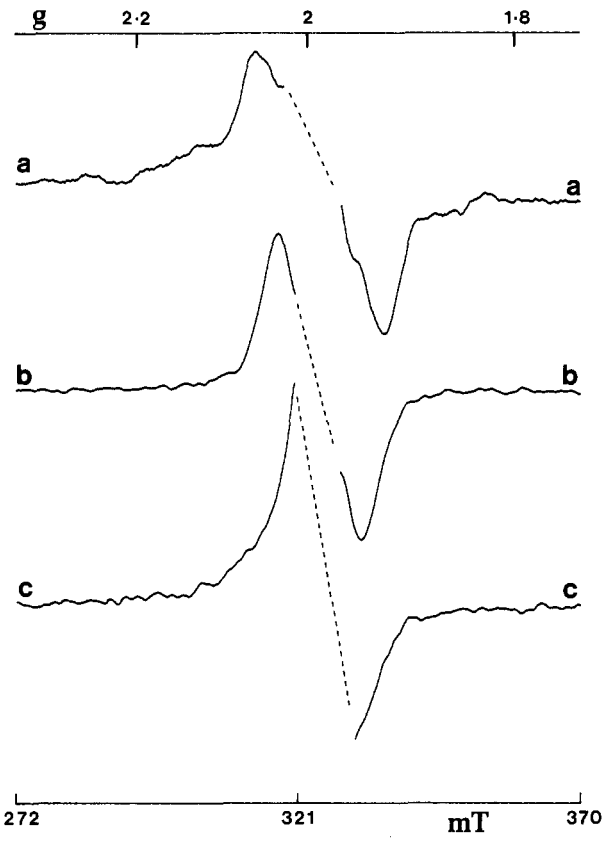

FIGURE 7: EPR spectra comparing the ling shapes of the three types of S3 signals. Samples contained 0.5 mM PPBQ and 0.3 M sucrose. Samples were illuminated for 30 s and frozen under illumination to 77 K, and the 30-min, 273 K dark-adapted spectrum was subtracted to give the difference spectrum shown. Samples were treated as follows: (a) PS2 treated with 300 mM calcium acetate at pH 5.5; (b) NaCl-washed, calcium-depleted sample reconstituted with extrinsic polypeptides, containing 5 mM EGTA at pH 6.5; and (c) PS2 treated with 100 mM ammonium chloride at pH 7.5. EPR conditions were as in Figure 3.

strontium chloride to an acetate-treated sample produced an S3 signal of narrow line width (Figure 6d) resembling that obtained by ammonia treatment (see Figure 7) or by chloride depletion (Baumgarten et al., 1990; Boussac et al., 1992). The line at $g = 1.9$ in Figure 6d probably represents an increased yield of Q_A iron semiquinone in this sample.

In summary, the study of additions of various cation chlorides and acetates indicate that S3 signals can be assigned to three types on the basis of line shape properties. These are shown in Figure 7. Figure 7 shows the broad line width with complex line shape obtained by acetate treatment (Figure 7a), the simpler line shape and smaller line width obtained by calcium depletion in the presence of chloride (Figure 7b) and the narrow line width produced by ammonia (Figure 7c), strontium treatment (Figure 6d), or chloride depletion and fluoride treatment (Baumgarten et al., 1990; Boussac et al., 1992). Some treatments result in mixtures of these forms, producing more complex line shapes.

DISCUSSION

There is now an accumulation of evidence to show that the OEC can exhibit a number of structural forms in a particular S state such as S_2. These appear to be influenced by (a) the type of cation cofactor bound, (b) the type of anion bound, (c) substrate analogues such as ammonia, (d) protonation, and (e) the binding of the 17- and 23-kDa polypeptides.

Various treatments that perturb calcium and/or chloride binding cause the OEC to be blocked one turnover beyond S_2, allowing the proposed S_2X^+ interaction (S3, X = organic radical) to be observed by EPR [see Debus (1992) and Rutherford et al. (1992)]. In all samples which show an S3-type signal, the normal S_2 state is perturbed, either favoring other forms of S_2 such as the $g = 4.1$ form and/or altering the line shape and stability of the multiline form. We have demonstrated above that an alteration of the properties of S_2 also occurs in acetate-treated samples, confirming earlier EPR and thermoluminescence measurements (Ono et al., 1987). The difficulty in observing a multiline-type S_2 signal in acetate-treated samples is probably due to changes in stability, i.e., redox potential and/or the structure of the cluster, which alter the magnetic properties of the S_2 state.

The data presented above also reveal that acetate treatment at pH 5.5 produces a new more complex type of S3 EPR signal in PS2 samples. It is proposed that the effects are caused by two linked processes, displacement of chloride and binding of acetate, though not necessarily at the same site. The results demonstrate that the effect of cations and anions on the S3 EPR signal can be compared and studied by a relatively simple method using high concentrations of the ion at the appropriate pH.

The assignment of the S3 signal to an organic radical magnetically interacting (exchange and/or dipolar coupled) with the manganese cluster (Boussac et al., 1989; Sivaraja et al., 1989), i.e., an interaction between an $S = {}^1/_2$ radical and the $S' = {}^1/_2$ S_2 state (Boussac et al., 1990b) suggests that changes in splitting (i.e., magnetic coupling), involve slight

structural differences between the interacting species. The observation of the outer peaks in acetate-treated samples suggest an increase in magnetic coupling (probably the exchange interaction) between the two species, relative to calcium-depleted samples. This would give two sets of lines with a common midpoint, weaker outer lines, and approximately equal separation between lines, which is close to the experimental observation. In the simulation of the S3 signal (Boussac et al., 1990b), a weak electron exchange interaction between an organic radical and the $S' = {}^1/_2 S_2$ state simulated the signal. A broad radical was needed for the simulation, indicating weak dipolar character. The weak interaction suggests that the radical probably is not directly liganded to the manganese cluster, but such a binding may be possible if the manganese cluster occurs as a dimer of dimers and the radical is liganded to a manganese pair only weakly contributing to the $S' = {}^1/_2 S_2$ state. In the acetate-treated samples we are unsure of the line shape of both the organic radical and the signal from the OEC, so other explanations for the signal are possible. The signal could even arise from the manganese cluster alone.

There have been two suggestions for the organic radical proposed to be involved, histidine (Boussac et al., 1990b) and tyrosine (Hallahan et al., 1992). The assignment of S3 to an interaction between the manganese cluster and a histidine radical rests on the interpretation of the optical spectrum obtained by Boussac et al. (1990b). As outlined by Debus (1992), the assignment of the organic radical to histidine was done by comparison with the absorption spectrum of a histidine–hydroxy adduct obtained by pulse radiolysis at pH 9.2 and not His^+, which weakens this assignment.

Bock et al. (1988) observed a 1.4-mT radical in acetate-treated PS2 under certain conditions. It was interpreted as being due to a broadened $P680^+$ but has also been suggested to be involved in an interaction with the histidine radical (Boussac et al., 1992). The 1.4-mT radical was formed when Y_z^+ was maintained in an oxidized state using a rapid repetition of laser flashes. It had a faster decay rate than Y_z^+. It was therefore probably not a component between Y_z and the OEC and was perhaps an altered form of Y_z or alternative donor to P680 [see Miller and Brudvig (1991)].

Hallahan et al. (1992) observed an increased yield of tyrosine radical at cryogenic temperatures under conditions which trap the S3 signal and attributed this to the trapping of Y_z^+. Boussac and Rutherford (1992) argued that the increased size of tyrosine radical was due to changes in the relaxation behavior of Y_D^+. This could not be distinguished from a mixture of Y_z^+ and Y_D^+, which would also have faster relaxation properties. However, if correct, assigning the changes to Y_D^+ alone simplifies the proposals of Hallahan et al. (1992) by removing the need to account for a noninteracting population of Y_z^+ at cryogenic temperatures. A further consequence is that the S3 state would be significantly different from the native S_3 state, as it was previously reported that Y_D^+ had a very similar microwave power saturation behavior in native S_2 and S_3 (Styring & Rutherford, 1988).

In Hallahan et al. (1992) a high proportion of centers in calcium-depleted samples generated Y_z^+ at room temperature, in contrast with the low yield obtained by Boussac et al. (1992) in kinetic EPR measurements. It is possible that slowly decaying Y_z^+ may have remained oxidized in the experiments of Boussac et al. (1992), leading to a decreased yield per laser flash. Significant yields of Y_z^+ have also been reported in ammonia-treated, chloride-depleted, and now acetate-treated samples, each of which shows S3-type EPR signals [Yocum & Babcock, 1981; Bock et al., 1988; Hallahan et al., 1992; see Debus (1992) for review]. Calcium depletion has also been shown to slow the kinetics of reduction of photooxidized Y_z^+ by the Mn cluster (Ghanotakis et al., 1984; Dekker et al., 1984; Ono & Inoue, 1989) with the conclusion that low-pH citrate "calcium-depleted" samples are affected between the OEC and Y_z^+ (Ono & Inoue, 1989; Ono et al., 1991). It is therefore clear that substantial amounts of Y_z^+ are observed in these inhibited samples. What is still unclear is if Y_z^+ is involved in the S3 signal. The oxidation of another amino acid or the manganese cluster via Y_z^+ could occur. The correlation of a slowing of the decay of Y_z^+ and ability to generate S3 signals may be a coincidence, but the possibility that Y_z^+ and a modified form of S_2 interact to give the S3 EPR signal remains.

The S_2X^+ interpretation of the S3 signal assumes the lack of oxidation of manganese on the S_2 to S_3 step. This has been supported by EXAFS (Guiles et al., 1990), EPR relaxation studies (Styring & Rutherford, 1988; Evelo et al., 1989), and magnetic susceptibility measurements (Baumgarten et al., 1990) and by some interpretations of optical and NMR studies [see Debus (1992) and Rutherford et al. (1992) for reviews]. A recent paper (Ono et al., 1992) has, however, indicated an oxidation of manganese on the native S_2 to S_3 step. This suggests that the EPR data on the inhibited samples may be explained as formation of modified S_3 by manganese oxidation via Y_z^+ but at a rate that allows a significant population of S_2 Y_z^+ to exist. The resolution of the origin of the S3 signal must, however, await confirmation of the changes to manganese on the S_2 to S_3 step and the availability of better optical data.

ACKNOWLEDGMENT

We wish to thank Professor Joseph Warden and Dr. Stephen Rigby for helpful comments and discussion.

REFERENCES

Andreasson, L.-E., & Lindberg, K. (1992) *Biochim. Biophys. Acta 1100*, 177–183.
Baumgarten, M., Philo, J. S., & Dismukes, G. C. (1990) *Biochemistry 29*, 10814–10822.
Berthold, D. A., Babcock, G. T., & Yocum, C. F. (1981) *FEBS Lett. 134*, 231–234.
Blubaugh, D., & Govindjee (1988) *Photosynth. Res. 19*, 85–128.
Bock, C. H., Gerken, S., Stehlik, D., & Witt, H. T. (1988) *FEBS Lett. 227*, 141–146.
Boussac, A., & Rutherford, A. W. (1988) *Biochemistry 27*, 3476–3483.
Boussac, A., & Rutherford, A. W. (1992) *Biochemistry 31*, 7441–7445.
Boussac, A., Zimmerman, J. L., & Rutherford, A. W. (1989) *Biochemistry 28*, 8984–8989.
Boussac, A., Zimmerman, J. L., & Rutherford, A. W. (1990a) *FEBS Lett. 277*, 69–74.
Boussac, A., Zimmerman, J. L., Rutherford, A. W., & Lavergne, J. (1990b) *Nature 347*, 303–306.
Boussac, A., Setif, P., & Rutherford, A. W. (1992) *Biochemistry 31*, 1224–1234.
Britt, R. D., Zimmerman, J. L., Sauer, K., & Klein, M. P. (1989) *J. Am. Chem. Soc. 111*, 3522–3532.
Buser, C. A., Diner, B. A., & Brudvig, G. W. (1992) *Biochemistry 31*, 11449–11459.
Casey, J. L., & Sauer, K. (1984) *Biochim. Biophys. Acta 767*, 21–28.
Coleman, W. J. (1990) *Photosynth. Res. 23*, 1–27.
Damoder, R., Klimov, V. V., & Dismukes, G. C. (1986)

Biochim.Biophys. Acta 848, 378–391.
Debus, R. J. (1992) *Biochim. Biophys. Acta 1102*, 269–352.
Debus, R. J., Barry, B. A., Babcock, G. T., & McIntosh, L. (1988a) *Proc. Natl. Acad. Sci. U.S.A. 85*, 427–430.
Debus, R. J., Barry, B. A., Sithole, I., Babcock, G. T., & McIntosh, L. (1988b) *Biochemistry 27*, 9071–9074.
de Paula, J. C., Li, P. M., Miller, A.-F., Wu, B. W., & Brudvig, G. W. (1986) *Biochemistry 25*, 6487–6494.
Dismukes, G. C., & Siderer, Y. (1980) *FEBS Lett. 121*, 78–80.
Evelo, R. G., Styring, S., Rutherford, A. W., & Hoff, A. J. (1989) *Biochim. Biophys. Acta 973*, 428–442.
Ford, R. C., & Evans, M. C. W. (1983) *FEBS Lett. 160*, 159–163.
Gerken, S., Dekker, J. P., Schlodder, E., & Witt, H. T. (1989) *Biochim. Biophys. Acta 977*, 52–61.
Ghanotakis, D. F., Yerkes, C. T., & Babcock, G. T. (1982) *Biochim. Biophys. Acta 682*, 21–31.
Ghanotakis, D. F., Babcock, G. T., & Yocum, C. F. (1984) *FEBS Lett. 167*, 127–130.
Guiles, R. D., Zimmermann, J. L., McDermott, A. E., Yachandra, V. K., Cole, J. L., Dexheimer, S. L., Britt, R. D., Wieghardt, K., Bossek, U., Sauer, K., & Klein, M. P. (1990) *Biochemistry 29*, 471–485.
Haddy, A., Dunham, W. R., Sands, R. H., & Aasa, R. (1992) *Biochim. Biophys. Acta 1099*, 25–34.
Hallahan, B. J., Nugent, J. H. A., Warden, J. T., & Evans, M. C. W. (1992) *Biochemistry 31*, 4562–4573.
Hanssum, B., Dohnt, G., & Renger, G. (1985) *Biochim. Biophys. Acta 806*, 210–220.
Homann, P. H. (1988) *Biochim. Biophys. Acta 94*, 1–13.
Kelley, P. M., & Izawa, S. (1978) *Biochim. Biophys. Acta 502*, 198–210.
Kim, D. H., Britt, R. D., Klein, M. P., & Sauer, K. (1992) *Biochemistry 31*, 541–547.
Kirilovsky, D. L., Boussac, A., van Mieghem, F. J. E., Ducruet, J.-M. R. C., Setif, P. R., Yu, J., Vermass, W. F. J., & Rutherford, A. W. (1992) *Biochemistry 31*, 2099–2107.
Kok, B., Forbush, B., & McGloin, M. (1970) *Photochem. Photobiol. 11*, 457–475.
Lockett, C. J., Demetriou, C., Bowden, S. J., & Nugent, J. H. A. (1990) *Biochim. Biophys. Acta 1016*, 213–218.
Maclachlan, D. J., Nugent, J. H. A., & Evans, M. C. W. (1992) in *Proceedings of the 9th International Congress on Photosynthesis* (Murata, N., Ed.) Vol. II, pp 373–376, Kluwer Academic Publishers, Dordrecht, The Netherlands.
Metz, J. G., Nixon, P. J., Rogner, M., Brudvig, G. W., & Diner, B. A. (1989) *Biochemistry 28*, 6960–6969.
Miller, A. F., & Brudvig, G. W. (1991) *Biochim. Biophys. Acta 1056*, 1–18.
Miyao, M., & Murata, N. (1984) *FEBS Lett. 168*, 118–120.
Nugent, J. H. A., Doetschman, D. C., & Maclachlan, D. J. (1992) *Biochemistry 31*, 2935–2941.
Ono, T., & Inoue, Y. (1989) *Biochim. Biophys. Acta 973*, 443–449.
Ono, T., & Inoue, Y. (1990a) in *Current Research in Photosynthesis* (Baltscheffsky, M., Ed.) Vol. I, pp 741–744, Kluwer Academic Publishers, Dordrecht, The Netherlands.
Ono, T., & Inoue, Y. (1990b) *Biochim. Biophys. Acta 1020*, 269–277.
Ono, T., Zimmermann, J. L., Inoue, Y., & Rutherford, A. (1986) *Biochim. Biophys. Acta 851*, 193–201.
Ono, T., Nakayama, H., Gleiter, H., Inoue, Y., & Kawamori, A. (1987) *Arch. Biochem. Biophys. 256*, 618–624.
Ono, T., Kusunoki, M., Matsushita, T., Oyanagi, H., & Inoue, Y. (1991) *Biochemistry 30*, 6836–6841.
Ono, T., Noguchi, T., Inoue, Y., Kusunoki, M., Matsushita, T., & Oyanagi, H. (1992) *Science 258*, 1335–1337.
Pauly, S., Schlodder, E., & Witt, H. T. (1992) *Biochim. Biophys. Acta 1090*, 203–210.
Renger, G. (1972) *Biochim. Biophys. Acta 256*, 428–439.
Rutherford, A. W., Zimmermann, J. L., & Boussac, A. (1992) in *The Photosystems: Structure, Function and Molecular Biology* (Barber, J., Ed.) Chapter 5, pp 179–229, Elsevier Science Publishers, Amsterdam.
Sandusky, P. O., & Yocum, C. F. (1986) *Biochim. Biophys. Acta 849*, 85–93.
Saygin, O., Gerken, S., Meyer, B., & Witt, H. T. (1986) *Photosynth. Res. 9*, 71–78.
Sinclair, J. (1984) *Biochim. Biophys. Acta 764*, 247–252.
Sivaraja, M., Tso, J., & Dismukes, G. C. (1989) *Biochemistry 28*, 9459–9464.
Stemler, A., & Murphy, J. B. (1985) *Plant Physiol. 77*, 974–77.
Styring, S. A., & Rutherford, A. W. (1987) *Biochemistry 26*, 2401–2405.
Styring, S. A., & Rutherford, A. W. (1988) *Biochemistry 27*, 4915–4923.
Theg, S. M., & Homann, P. H. (1982) *Biochim. Biophys. Acta 679*, 221–234.
Tso, J., Sivaraja, M., Philo, J. S., & Dismukes, G. C. (1991) *Biochemistry 30*, 4740–4747.
Vermaas, W. F. J., & Rutherford, A. W. (1984) *FEBS Lett. 175*, 243–248.
Vermaas, W. F. J., Renger, G., & Dohnt, G. (1984) *Biochim. Biophys. Acta 764*, 194–202.
Vermaas, W. F. J., Rutherford, A. W., & Hansson, O. (1988) *Proc. Natl. Acad. Sci. U.S.A. 85*, 8477–8481.
Warden, J. T., Blankenship, R. F., & Sauer, K. (1976) *Biochim. Biophys. Acta 423*, 462–478.
Yocum, C. F. (1991) *Biochim. Biophys. Acta 1059*, 1–15.
Yocum, C. F. & Babcock, G. T. (1981) *FEBS Lett. 130*, 99–102.